JACS
JOURNAL OF THE AMERICAN CHEMICAL SOCIETY

COMMUNICATION

pubs.acs.org/JACS

Single-Chain Folding of Polymers for Catalytic Systems in Water

Takaya Terashima, Tristan Mes, Tom F. A. De Greef, Martijn A. J. Gillissen, Pol Besenius, Anja R. A. Palmans,* and E. W. Meijer*

Institute for Complex Molecular Systems, Laboratory of Macromolecular and Organic Chemistry, Laboratory of Chemical Biology, Eindhoven University of Technology, P.O. Box 513, 5600 MB Eindhoven, The Netherlands

Supporting Information

ABSTRACT: Enzymes are a source of inspiration for chemists attempting to create versatile synthetic catalysts. In order to arrive at a polymeric chain carrying catalytic units separated spatially, it is a prerequisite to fold these polymers in water into well-defined compartmentalized architectures thus creating a catalytic core. Herein, we report the synthesis, physical properties, and catalytic activity of a water-soluble segmented terpolymer in which a helical structure in the apolar core is created around a ruthenium-based catalyst. The supramolecular chirality of this catalytic system is the result of the self-assembly of benzene-1,3,5-tricarboxamide side chains, while the catalyst arises from the sequential ruthenium-catalyzed living radical polymerization of the different monomers followed by ligand exchange. The polymers exhibit a two-state folding process and show transfer hydrogenation in water.

Organic chemistry in water is one of the cornerstones of today's endeavor for a sustainable society. Both water-soluble catalysts and enzymes are frequently used in modern organic synthesis. Whereas most of the water-soluble synthetic catalysts have their active site exposed to the aqueous solution,[1,2] enzymes generally make use of a compartmentalized hydrophobic cavity within the structure, which has a hydrophilic outer shell. This compartmentalization is achieved via a controlled primary sequence and single-chain folding to give an ordered tertiary architecture using the preferred conformation of chain segments (α-helix, β-sheet).[3,4] The isolated well-defined interior allows efficient, selective catalysis. Inspired by their understanding of enzymes, chemists have designed a wide range of versatile, artificial catalysts. Catalysts based on star polymers[5−9] and dendrimers[10−14] represent synthetic macromolecules where catalytically active cores are isolated from the outer environment. However, these enzyme mimics rarely allow for efficient catalysis in water. Supramolecular folding of a single polymer chain[15−17] is, in turn, an intriguing possibility for the construction of well-defined catalytic systems exhibiting all the characteristics of enzymes. We have recently achieved single-chain folding of linear polymers bearing either *o*-nitrobenzyl protected 2-ureido-4[*1H*]-pyrimidinone (Upy) or benzene-1,3,5-tricarboxamide (BTA) side chains in apolar solvents via UV-mediated deprotection.[17,18] BTAs with chiral substituents are especially interesting to initiate a single polymer-chain folding process due to their efficient helical assembly with a preferred handedness in suitable solvents (Figure 1a).[19] Combining this helical motif with an amphiphilic sequenced terpolymer comprising an efficient catalytically active hydrophobic cavity would open new vistas for catalysis in water, the next step in polymer supported catalysis.[20,21] In this paper, we disclose a compartmentalized catalyst that catalyzes carbonyl reductions in water and describe in detail the folding process of this catalytic system.

Due to its high tolerance, ruthenium-catalyzed living radical polymerization (LRP)[22] allows for a one-pot synthesis of water-soluble random copolymers carrying hydrophilic poly(ethylene glycol) (PEG) and hydrophobic chiral BTA substituents, as well as water-soluble segmented terpolymers carrying catalytic sites in addition to the PEG and BTA substituents. The water-soluble random copolymers (PEGMA/BTAMA copolymers **P1**−**7**: Figure 1b) were synthesized in high yield (>90%) by Ru(Ind)Cl-$(PPh_3)_2$-catalyzed copolymerization of chiral BTA-bearing methacrylate (BTAMA) and poly(ethylene glycol) methyl ether methacrylate (PEGMA) with different PEG lengths. Copolymers with narrow molecular weight distributions ($M_w/M_n \approx 1.2-1.3$) and number-average molecular weights (M_n) in the range of 34 000−59 800 were obtained, as determined by size exclusion chromatography [SEC with poly(methyl methacrylate) standards]. The M_n's determined by proton nuclear magnetic resonance (^{1}H NMR) spectroscopy were in good agreement with those calculated from the monomer feed ratio to the initiator and the conversion (Figure S1, Table S1, Supporting Information). Copolymer **P4** with 20% BTA content showed typical infrared signals, corresponding to 3-fold, helical hydrogen bonding between the neighboring BTA molecules in the solid state (Figure S2). To place catalytic functions in the desired sites of the copolymers, we employed a one-pot method, in which $RuCl_2(PPh_3)_3$-catalyzed LRP is coupled with diphenylphosphinostyrene (SDP)[6,7] to simultaneously induce a ligand-exchange reaction with the catalyst. Here we applied this method to sequential segmentation in order to prepare water-soluble terpolymer **P8** carrying BTA substituents and catalytic sites (Figure 1c). After the copolymerization of PEGMA and BTAMA reached around 50% conversion, SDP and a fresh Ru-catalyst were directly added into the solution (Figure S3). Interestingly, a rapid and complete conversion of SDP was observed which was followed by the full consumption of the remaining methacrylates. The purified polymer (M_n = 35 200 $M_w/M_n \approx 1.5$) was red-brown and the UV−vis spectrum was similar to that of $RuCl_2(PPh_3)_3$, demonstrating that SDP efficiently entrapped ruthenium onto the copolymers via the ligand-exchange reaction

Received: January 17, 2011
Published: March 15, 2011

dx.doi.org/10.1021/ja2004494 | *J. Am. Chem. Soc.* 2011, 133, 4742–4745

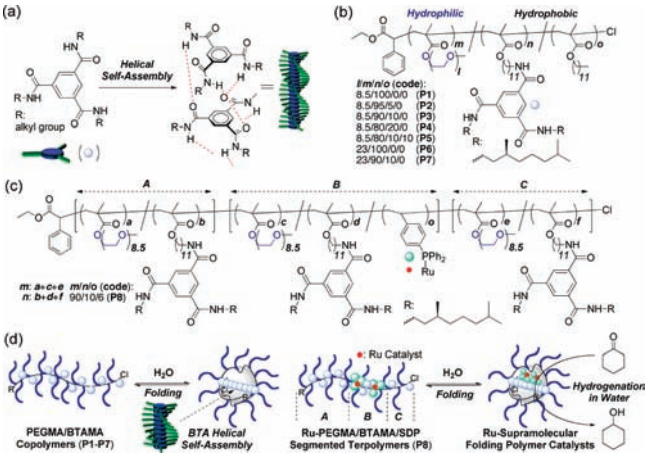

Figure 1. (a) Helical self-assembly of chiral BTAs via 3-fold hydrogen bonding. Design of water-soluble chiral polymers for supramolecular folding in water: (b) PEGMA/BTAMA copolymers (**P1**−**P7**) with ***l*** = average number of glycol units, ***m*** = average number of PEGMA units, ***n*** = average number of BTAMA units, and ***o*** = average number of dodecyl methacrylate units; (c) Ru-PEGMA/BTAMA/SDP segmented terpolymer **P8**. (d) Supramolecular single-chain folding of polymers in water affording a compartmentalized catalyst for the transfer hydrogenation of ketones.

during the polymerization (Figure S3D). The number of ruthenium atoms was estimated at 2.5 per chain by inductively coupled plasma atomic emission spectroscopy (ICP-AES: polymer-bound Ru = 50 μmol/g-polymer); an almost quantitative incorporation of the fed catalyst. Similarly as above, the characterization of the sequence-controlled terpolymer **P8** is in full agreement with the structure assigned (Table S1, Figure S3).

As a result of the hydrophilic PEG side chains, all (co)polymers **P1**−**P8** are soluble in water. Since hydrophobic and hydrogen-bonding BTA units are randomly incorporated into the side chains, these copolymers are expected to form compact conformations via the intramolecular self-assembly of the BTA moieties in water. Thus, the polymers were analyzed by SEC, dynamic and static light scattering (DLS and SLS), multi-angle laser light scattering coupled with SEC (SEC-MALLS), diffusion ordered spectroscopy (DOSY), and small-angle X-ray scattering (SAXS) (Tables S2−S5, Figures S4−S7). SEC in water and DMF (PEG standards) showed unimodal peaks with narrow M_w/M_n ratios for both **P6** (without BTA moieties) and **P7** (with 10% BTA moieties) (Figure 2a). Interestingly, in water the peak top and number average molecular weight of the copolymer (**P7**) are smaller (~10 kg/mol) than those of the homopolymer (**P6**), while they show similar molecular weights in DMF. This suggests that the hydrodynamic radius (R_h) of **P7** is strongly affected by the nature of the solvent, water or DMF. On the other hand, the *absolute* weight average molecular weights of the copolymer (**P7**) are similar in water (M_w = 146 000 determined by SLS) and DMF (M_w = 149 000 determined by SEC-MALLS) (Table S2). DLS measurements in water at 1 mg/mL (Table S3) confirm that the R_h of **P7** is smaller than that of **P6** (R_h = 6.8 and 7.8 nm for **P7** and **P6**, respectively). The copolymer maintained a smaller size than the homopolymer, independent of the temperature between 25 and 60 °C and the concentration (1.0−5.0 mg/mL). The compact conformation in water of **P7** in contrast to **P6** was further supported by SAXS measurements of the two samples in terms of the radius of

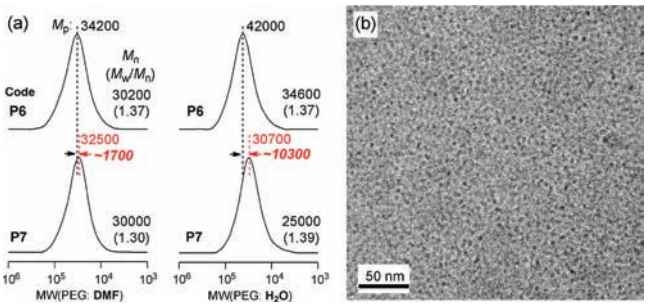

Figure 2. (a) SEC analysis of **P6** and **P7** in water and DMF; all molecular weights are given in g/mol and determined with respect to PEG standards. (b) Cryo-TEM images of **P8** ($M_{w,SLS}$ = 105,000, $R_{h,DLS}$ = 6.8 nm): Magnification = 62 k.

gyration (R_g) and the excluded volume parameter (ν) (R_g = 6.7 nm and ν = 0.253 for **P7**, R_g =8.5 nm and ν = 0.368 for **P6**) (Figure S6, Table S4). Similar to the case of **P7**, all copolymers with 5 to 10% BTA units (**P2**, **P3**, **P5**, **P8**) fold into compact conformations of nanosize dimensions in water. They all show almost the same absolute weight average molecular weights (M_w) in water and DMF and small R_h's (4.8−6.8 nm) with narrow polydispersities as determined by DLS in water (Tables S2, S3). Additionally, the R_h of the PEGMA/BTAMA copolymers (**P3**: 10% BTA; 8.5 PEG) by DLS in water is very close to the one determined by ^{1}H DOSY NMR in D_2O [R_h (DLS) = 5.3 nm, R_h (DOSY) = 5.2 nm] (Figure S7). Cryogenic transmission electron microscopy (cryo-TEM) is also a powerful characterization technique thanks to the high contrast of the nanoparticles' hard helical core in vitrified water. The BTA-rich part of the (co)polymers can be directly observed as black dots by cryo-TEM (Figures 2b, S8). Typically, **P8** almost uniformly showed nanoparticles of around 3 to 4 nm diameter, without any intermolecular aggregation. The observed dots probably indicate the hydrophobic cores of the core−shell-like structures, due to the low contrast of the swollen hydrophilic shell in water. These results demonstrate that the PEGMA/BTAMA copolymers with and without Ru-catalytic sites form single-chain nanoparticles in water and that there is no intermolecular aggregation. The collapse is proposed to be the result of the folding through hydrogen-bonding interactions of the BTA pendant groups within the hydrophobic compartment (Figures 1d, S9).

For studying the folding process of the single-chain nanoparticles, we made use of the stereochemical probe introduced into the self-assembling BTA unit. The PEGMA/BTAMA copolymer **P3** in water was investigated with temperature-dependent Circular Dichroism (CD) spectroscopy at 10 K intervals between 273 and 363 K (Figure 3a) and temperature-dependent UV−vis (Figure S10). **P3** exhibits a bisignate Cotton effect identical to that previously observed for the helical BTA self-assembly in alkane solvents (C_{BTA} = 50 μM) demonstrating that even in water helical stacks stabilized by 3-fold hydrogen bonding are formed.[18,19] The negative Cotton effect at 225 nm decreased upon heating the solution from 273 to 363 K, and the solution finally turned turbid due to the lower critical solution temperature (LCST) of the PEG chains above 358 K. Full reversibility without hysteresis was observed upon slow cooling (Figure S11). While all BTA-bearing copolymers **P2**−**5** and **P7**,**8** exhibit CD spectra of similar shape in water at 293 K (C_{BTA} = 50 μM) (Figure 3b, Figure S12−S16), the polymer composition, PEG chain length, BTA concentration, and addition of denaturing

dx.doi.org/10.1021/ja2004494 |*J. Am. Chem. Soc.* 2011, 133, 4742–4745

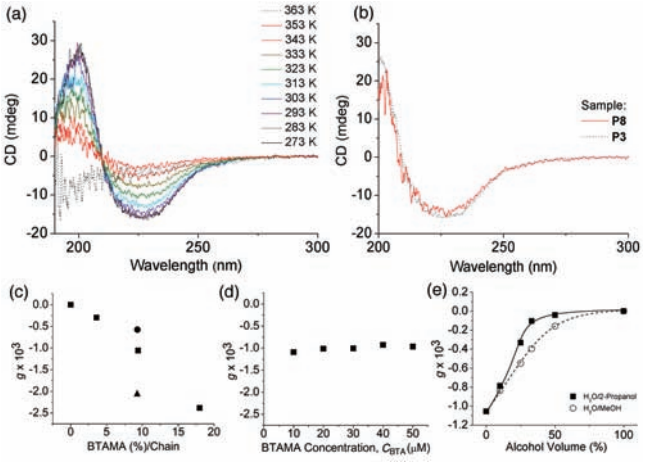

Figure 3. Supramolecular folding of PEGMA/BTAMA-based copolymers in water: (a) Temperature-dependent CD spectra of **P3** in water (BTAMA concentration: C_{BTA}, 50 μM) from 273 to 363 K with 10 K intervals; (b) CD spectra of **P8** and **P3** in H_2O (C_{BTA}: 50 μM) at 293 K; (c) Anisotropy value (g) of PEGMA/BTAMA copolymers [filled square: **P1**, **P2**, **P3**, **P4**; filled circle: **P7**; filled triangle: **P5**; C_{BTA} = 50 μM] in H_2O at 293 K as a function of the BTAMA content (%) per single chain, monitored at λ = 225 nm; (d) g of **P3** in H_2O at 293 K as a function of C_{BTA} (10−50 μM), monitored at λ = 225 nm; (e) g of **P3** (C_{BTA} = 50 μM) in H_2O/alcohol (0/100−100/0, v/v) at 293 K, monitored at λ = 225 nm.

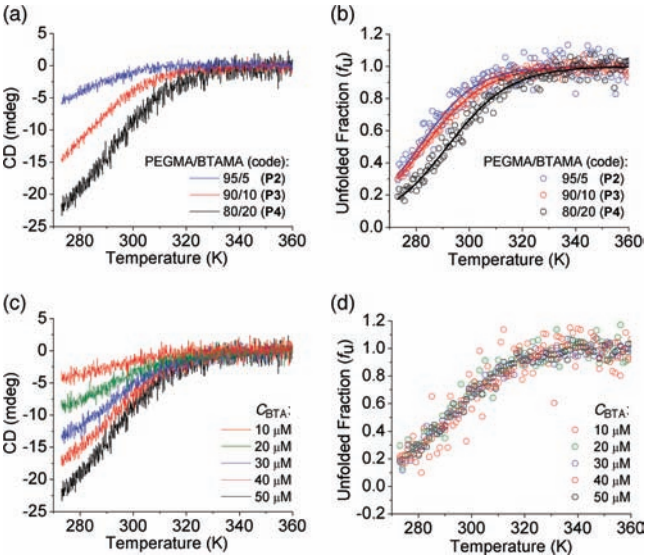

Figure 4. Two-state folding model analysis: (a) CD cooling curves of **P2**, **P3**, **P4** (C_{BTA} = 50 μM) monitored at λ = 225 nm in H_2O/2-propanol (3/1, v/v) at temperatures from 363 to 273 K (cooling rate: −1 K/min) and (b) the unfolded fraction (f_u: open circles) fitted by two state model (solid lines); (c) CD cooling curves of **P4** (C_{BTA} = 10−50 μM) monitored at λ = 225 nm in H_2O/2-propanol (3/1, v/v) at temperatures from 363 to 273 K (cooling rate: −1 K/min) and (d) the f_u (open circles).

alcohol affect the magnitude of the Cotton effect. The absolute anisotropy value (g) of the negative Cotton effect at 225 nm increases in the series **P2**, **P3**, **P4** with BTA contents of 5, 10, 20% per chain, respectively (Figure 3c). Interestingly, g is independent of total BTA concentration (C_{BTA} = 10−50 μM) in **P3** (Figures 3d, S13). Both observations indicate that the *local* BTA concentration is responsible for the magnitude of the Cotton effect and that the self-assembly occurs within a single chain. In addition, g increases by the additional copolymerization of dodecyl methacrylate in **P5** and decreases by the introduction of longer PEG side chains as in the case of **P7** (Figure 3c). The importance of hydrophobicity was further revealed by temperature-dependent CD measurements of **P3** in mixed solvents of water and 2-propanol (H_2O/2-propanol = 100/0−0/100, v/v) from 363 to 273 K, monitored at 225 nm (Figure S14). The anisotropy value g at 293 K decreases with the increasing ratio of 2-propanol to water (Figure 3e), which was even more apparent at higher temperatures. Methanol also decreases the Cotton effects of the pendant BTAs in **P3**, but to a lesser extent.

Additional evidence that an *intra*molecular folding process is responsible for the formation of single-chain nanoparticles was gathered by quantitative analysis of the temperature-dependent CD spectra. Previously, we disclosed that the *inter*molecular self-assembly of BTAs in apolar solvents via 3-fold hydrogen bonding (Figure 1a) follows a cooperative growth mechanism characterized by asymmetric and nonsigmoidal melting curves.[19] These nonsigmoidal melting curves show typical concentration-dependent elongation temperatures (T_e) at which rapid intermolecular growth of the BTA assemblies occurs. In sharp contrast, the melting curves of the PEGMA/BTAMA copolymers do not exhibit a clear elongation temperature (Figures 4a, S11). In fact, the melting curves of the PEGMA/BTAMA copolymers are reminiscent of those obtained by the thermal denaturation of *intra*molecularly folded proteins and peptides.[23] The thermal unfolding processes of proteins and peptides can be analyzed using a two-state folding model in which folded and unfolded populations are in thermal equilibrium. We successfully applied (Figures S17, S18; Tables S6−S8) this model to the PEGMA/BTAMA copolymers **P2**, **P3**, **P4** (C_{BTA} = 50 μM) to probe the effects of local BTA concentration (Figure 4a, b) as well as total BTA concentration (**P4**: C_{BTA} = 10−50 μM) (Figure 4c, d) in H_2O/2-propanol (3/1, v/v). The model analysis revealed that the melting temperature (T_m) increases with increasing local BTA concentration [T_m = 280 (**P2**), 283 (**P3**), 293 (**P4**) K] and is independent of the total BTA concentration [T_m = ∼293 K: C_{BTA} (**P4**) = 10−50 μM]. In addition, the model allows us to derive the change in the heat capacity, ΔC_p, during the unfolding which is positive for all polymers **P2**−**P4** (Table S8). Positive values for ΔC_p are characteristic for the thermal denaturation of globular proteins and are associated with exposure of the hydrophobic groups to the polar environment.[24] This observation adds to our hypothesis that the folding of the PEGMA/BTAMA copolymers in water based media is associated with the formation of a hydrophobic compartment.

The results gathered from the CD data strongly support the proposal of a hydrophobic compartment in the PEGMA/BTAMA-based copolymers in water, where the self-assembly of the BTA pendant groups efficiently creates a helical secondary structure with a preferred handedness. To examine the feasibility of a catalyst embedded in the hydrophobic cavity created by the folding of BTA units as a reaction space for aqueous catalysis, we selected Ru-catalyzed transfer hydrogenations as a model system. We performed the transfer hydrogenation of partially water-soluble cyclohexanone coupled with HCOONa as the hydrogen source at 40 °C (Figure 1d) and using PEGMA/BTAMA/SDP terpolymer **P8** as the catalyst.[25] **P8** exhibits the same CD spectra (in both shape and intensity at every temperature: Figures 3b and

dx.doi.org/10.1021/ja2004494 |*J. Am. Chem. Soc.* 2011, 133, 4742–4745

S15) in water as observed for **P3**. Moreover, in the presence of 0.4 M HCOONa and in a dilute solution comprising either cyclohexanone or cyclohexanol, helical folding was observed for **P8** indicating that BTA self-assembly is stable in conditions under which catalysis is performed (Figure S16). The folded polymer homogeneously and quantitatively catalyzed the reduction of cyclohexanone to cyclohexanol (18 h, [substrate]/[Ru] = 200/1) (Table S9). Even at low catalyst feed ratios ([substrate]/[Ru] = 1000/1), the polymer efficiently induced the catalysis (conversion of 98% in 50 h). Similar results were obtained with acetophenone, which is poorly water-soluble, as the substrate (18 h, conversion = 86%). The turnover frequencies observed in our system ($10-20\ h^{-1}$) compare well to those of reported water-soluble Ru-complexes ($1-40\ h^{-1}$) obtained under similar conditions although an exact comparison is difficult as a result of the different ligands employed.[25−30] Thus, dissolving **P8** in water suffices to prepare a compartmentalized system capable of transfer hydrogenations as a result of the formed hydrophobic cavity. The excellent activity arises from the solubility of **P8** in water due to the PEG chains and a catalyst that is located in a hydrophobic compartment. Gratifyingly, the folded catalytic system was neither decomposed nor hydrolyzed, as confirmed by ^{1}H NMR analysis.

The structural characterization of PEGMA/BTAMA copolymers by various scattering techniques combined with thermal behavior that follows a two-state folding process strongly supports the view that *intra*molecular folding of the pendant BTAs results in collapsed single-chain nanoparticles in a process very similar to the folding of proteins. Moreover, the folding is unaffected by the incorporation of a catalytically active Ru-complex. As a next step, we would like to couple the catalytically active unit to the internal chiral structure to achieve asymmetric synthesis.[31,32] The present system shows effective transfer hydrogenations with prochiral substrates such as acetophenone, but no enantiomeric preference is observed, as could be expected from the remote positioning of the chiral internal structure from the active site. Moreover, these novel catalytic systems will open new vistas for artificial enzyme-like organic chemistry in water, and possibilities for multistep synthesis in a single pot due to tandem catalysis with different folded catalytic polymers can be explored.

■ ASSOCIATED CONTENT

Ⓢ Supporting Information. Experimental details; characterization; SLS, DLS, SAXS, and DOSY data; cryo-TEM images; CD spectroscopy; and two-state model analysis. This material is available free of charge via the Internet at http://pubs.acs.org.

■ AUTHOR INFORMATION

Corresponding Author
a.palmans@tue.nl; e.w.meijer@tue.nl

■ ACKNOWLEDGMENT

This research was supported by The Netherlands Organization for Scientific Research (NWO) and the National Research School Catalysis (NRSC-C). We thank K. Fukae (Kyoto University) for SEC-MALLS; A. Terashima for SEC in water; A. M. Elemans-Mehring and J. L. J. van Dongen for ICP-AES; Dr. Guiseppe Portale for assistance with SAXS measurements; and Dr. R. Nicolaÿ, B, F. M. de Waal, and R. van der Weegen for the synthesis of BTAMA. We acknowledge Hokko Chemical (Japan) for the kind supply of diphenylphosphinostyrene (SDP). ESRF and NWO are acknowledged for providing beam time. T.T. is also grateful to the Kyoto University Foundation for grant-in-aid.

■ REFERENCES

(1) ten Brink, G.-J.; Arends, I. W. C. E.; Sheldon, R. A. *Science* **2000**, *287*, 1636–1639.
(2) Shaughnessy, K. H. *Chem. Rev.* **2009**, *109*, 643–710.
(3) Garcia-Viloca, M.; Gao, J.; Karplus, M.; Truhlar, D. G. *Science* **2004**, *303*, 186–195.
(4) Rose, G. D.; Fleming, P. J.; Banavar, J. R.; Maritan, A. *Proc. Natl. Acad. Sci. U.S.A.* **2006**, *103*, 16623–16633.
(5) Bosman, A. W.; Vestberg, R.; Heumann, A.; Fréchet, J. M. J.; Hawker, C. J. *J. Am. Chem. Soc.* **2003**, *125*, 715–728.
(6) Terashima, T.; Kamigaito, M.; Baek, K.-Y.; Ando, T.; Sawamoto, M. *J. Am. Chem. Soc.* **2003**, *125*, 5288–5289.
(7) Terashima, T.; Ouchi, M.; Ando, T.; Sawamoto, M. *J. Polym. Sci.: Part A, Polym. Chem.* **2010**, *48*, 373–379.
(8) Helms, B.; Guillaudeu, S. J.; Xie, Y.; McMurdo, M.; Hawker, C. J.; Fréchet, J. M. J. *Angew. Chem., Int. Ed.* **2005**, *44*, 6384–6387.
(9) Chi, Y.; Scroggins, S. T.; Fréchet, J. M. J. *J. Am. Chem. Soc.* **2008**, *130*, 6322–6323.
(10) Bosman, A. W.; Janssen, H. M.; Meijer, E. W. *Chem. Rev.* **1999**, *99*, 1665–1688.
(11) Grayson, S. M.; Fréchet, J. M. J. *Chem. Rev.* **2001**, *101*, 3819–3867.
(12) Helms, B.; Fréchet, J. M. J. *Adv. Synth. Catal.* **2006**, *348*, 1125–1148.
(13) Helms, B.; Meijer, E. W. *Science* **2006**, *313*, 929–930.
(14) Yu, J.; RajanBabu, T. V.; Parquette, J. R. *J. Am. Chem. Soc.* **2008**, *130*, 7845–7847.
(15) Hill, D. J.; Mio, M. J.; Prince, R. B.; Hughes, T. S.; Moore, J. S. *Chem. Rev.* **2001**, *101*, 3893–4011.
(16) Seo, M.; Beck, B. J.; Paulusse, J. M. J.; Hawker, C. J.; Kim, S. Y. *Macromolecules* **2008**, *41*, 6413–6418.
(17) Foster, E. J.; Berda, E. B.; Meijer, E. W. *J. Am. Chem. Soc.* **2009**, *131*, 6964–6966.
(18) Mes, T.; van der Weegen, R.; Palmans, A. R. A.; Meijer, E. W. *Angew. Chem., Int. Ed.* **2011**, accepted.
(19) Smulders, M. M. J.; Schenning, A. P. H. J.; Meijer, E. W. *J. Am. Chem. Soc.* **2008**, *130*, 606–611.
(20) Bergbreiter, D. E.; Tian, J.; Hongfa, C. *Chem. Rev.* **2009**, *109*, 530–582.
(21) Akiyama, R.; Kobayashi, S. *Chem. Rev.* **2009**, *109*, 594–642.
(22) Ouchi, M.; Terashima, T.; Sawamoto, M. *Chem. Rev.* **2009**, *109*, 4963–5050.
(23) Privalov, P. L. *Adv. Protein Chem.* **1979**, *33*, 167–241.
(24) Spolar, R. S.; Ha, J.-H.; Record, M. T., Jr. *Proc. Natl. Acad. Sci. U. S.A.* **1989**, *86*, 8382–8385.
(25) Wu, X.; Xiao, J. *Chem. Commun.* **2007**, 2449–2466.
(26) Liu, J.; Zhou, Y.; Wu, Y.; Li, X.; Chan, A. S. C. *Tetrahedron: Asymmetry* **2008**, *19*, 832–837.
(27) Li, X.; Wu, X.; Chen, W.; Hancock, F. E.; King, F.; Xiao, J. *Org. Lett.* **2004**, *6*, 3321–3324.
(28) Schlatter, A.; Kundu, M. K.; Woggon, W.-D. *Angew. Chem., Int. Ed.* **2004**, *43*, 6731–6734.
(29) Zeror, S.; Collin, J.; Fiaud, J.-C.; Zouioueche, L. A. *J. Mol. Catal. A* **2006**, *256*, 85–89.
(30) Arakawa, Y.; Chiba, A.; Haraguchi, N.; Itsuno, S. *Adv. Synth. Catal.* **2008**, *350*, 2295–2304.
(31) Yamamoto, T.; Suginome, M. *Angew. Chem., Int. Ed.* **2009**, *48*, 539–542.
(32) Boersma, A. J.; Klijn, J. E.; Feringa, B. L.; Roelfes, G. *J. Am. Chem. Soc.* **2008**, *130*, 11783–11790.